

Invited review

X-ray micro-computed imaging of wettability characterization for multiphase flow in porous media: A review

Shuangmei Zou^{1,2}, Chenhao Sun³✉*¹Key Laboratory of Theory and Technology of Petroleum Exploration and Development in Hubei Province, Wuhan 430074, P. R. China²Key Laboratory of Tectonics and Petroleum Resources, Ministry of Education, China University of Geosciences, Wuhan 430074, P. R. China³School of Minerals & Energy Resources Engineering, University of New South Wales, Kensington, NSW 2052, Australia**Keywords:**Wettability
X-ray microcomputed imaging
multiphase flow
contact angle
pore-scale physics**Cited as:**Zou, S., Sun, C. X-ray microcomputed imaging of wettability characterization for multiphase flow in porous media: A review. *Capillarity*, 2020, 3(3): 36-44, doi: 10.46690/capi.2020.03.01.**Abstract:**

With the advent of X-ray micro-computed tomography which is now routinely used, pore-scale fluid transport and processes can be observed in three-dimensional (3D) at the micro-scale. Multiphase flow experiments that are conducted under *in situ* imaging scanning conditions can be utilized to study the pore-scale physics relevant to subsurface technological applications. X-ray micro-tomographic imaging is a non-destructive technique for quantifying these processes in 3D within confined pores. This paper presents a review for the usage of X-ray micro-computed tomography experiments to investigate wettability effect on multiphase flow. The fundamental workflow of combining experiments with pore-scale *in situ* imaging scanning such as equipment requirements, apparatus design and fluid systems are firstly described. Then imaging analysis toolkit is presented for how to quantify interfacial areas, curvatures, contact angles, and fluid properties through these images. Furthermore, we show typical examples, illustrating recent studies for the wettability characterization by using X-ray micro-computed imaging.

1. Introduction

In the past two decades, X-ray imaging technique has been widely applied to investigate multiphase flow and transport in numerous natural and engineered processes such as ground water in environmental engineering, geological contaminant in soil science, oil recovery in petroleum engineering (Blunt et al., 2013; Armstrong et al., 2016). X-ray micro-computed tomography with the application for pore-scale physics during multiphase flow provides a nondestructive way to directly visualize the processes of subsurface flow and transport phenomena in porous media (Wildenschild and Sheppard, 2013). X-ray computed tomography has spatial resolution with micrometer for time-averaged phase distributions. Experimental studies by using X-ray imaging are able to quantify flow properties and transport mechanisms in rock samples which not only improve our current understanding of pore-scale physics in porous media, but also validate physically-based models that are capable of predicting fluid flow behaviors and transport properties (Karpyn et al., 2010; Georgiadis et al., 2013). Thus, the objective of this review is to provide an overview of

recent progresses in tomographic imaging using X-ray imaging technique integrated with laboratory facilities for wettability characterization during multiphase flow.

2. Combining flow experiments with imaging

With the advance of X-ray micro-computed tomography technique, it has become much more feasible to perform flow experiments on the scanning stage of imaging facility without disturbing fluid flow from transportation (Sheppard et al., 2014). For pore-scale multiphase flow obtaining spatial fluid distributions and saturations at the steady-state or quasi-static state during immiscible displacement, drainage/imbibition for capillary pressure or relative permeability measurement are burgeoning topics that have been widely discussed (Turner et al., 2004; Youssef et al., 2010; Reynolds and Krevor, 2015; Gao et al., 2017; Li et al., 2017; Reynolds et al., 2017). For multiphase flow experiments combined with X-ray microcomputed imaging, the systems need to reach at quasi-static equilibrium so that high quality images can be acquired during the scanning with minimal interfaces moving. Hence,

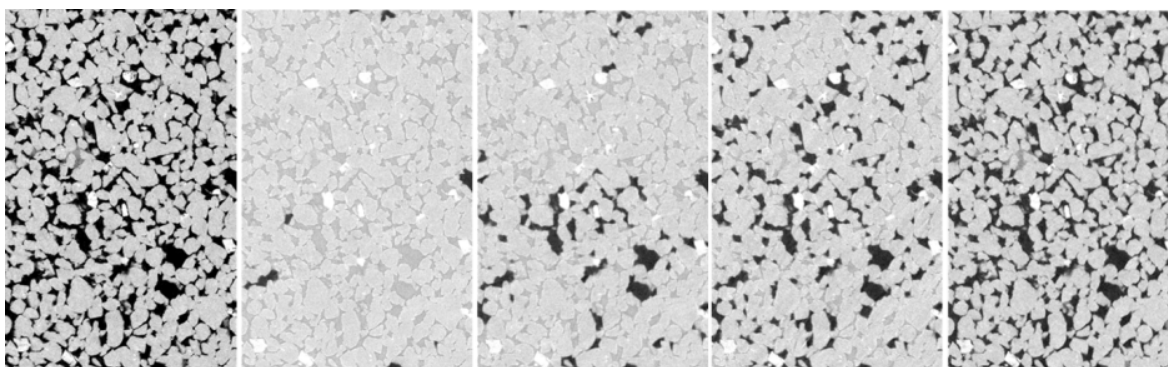


Fig. 1. This figure illustrates two-phase fluid distributions in a sandstone containing 2% percent of clay. The two-phase system is wetting phase (brine) and nonwetting phase (oil). results for partial wet images taken for 4 ratios. The images are taken during two-phase drainage flow. The core is firstly fully saturated with brine. Then brine and water are co-injected into the rock with decreasing water fractional flows. From left to right, they are dry image, water fractional flow: 0.9, 0.5, 0.1 and 0 wet images respectively. Dry image: black is pore space and grey is grain (white is mineral). Wet images: black is oil and dark grey is water and light grey is grain.

controlling the equilibrium state is important for imaging saturation states for multiphase flow system (Gao et al., 2017; Reynolds et al., 2017).

Multiphase flow experimental systems for laboratory core flooding are required for X-ray experimental imaging. With the introduction of X-ray absorbent dopants, contrast between multiphase fluids that present in the pore space has allowed a set of three-dimensional (3D) multiphase image data to be distinguished under *in situ* non-destructive imaging condition (Coles et al., 1998). For the wetting phase, it is doped with iodide such as KI or NaI or CsI. Several studies alternatively dope the non-wetting phase (oil phase) with n-dodecane (Feali et al., 2012) and iododecane (Hussain et al., 2014). The experimental system consists of a special designed core holder, injection fluid and production fluid systems. Imaging compatible Hassler-type core holders is built to perform multiphase flow experiments under image scanning conditions. The core holder must be adaptable to X-ray imaging facility with materials being transparent to X-ray. The whole core holder should have miniaturized size with lightweight so that high image resolution can be obtained which allows for more finely resolved analysis. The commonly used materials for flow cells are aluminum, titanium, Beryllium, polycarbonate, carbon fibre and polyetheretherketone (PEEK). Additionally, the attached fluid lines connected to core holder must be able to rotate 180° or even 360° with the sample rotated condition during imaging scanning. Multiple fluids under the flow are imaged which can be controlled by a high-precision syringe or piston pump, which provides precise injecting flowrates and targeted flow pressure. Under reservoir condition with high confining pressure, additional pumps are needed to supply confining fluid for the core holder. At outlet, production liquid is produced from fluid lines attached at core outlet and collected by a beaker.

3. Image acquisition, registration and segmentation

The standard process of acquiring *in situ* X-ray images for multiphase flow in porous media is similar to that in a

dry sample. The entire flow cell is rotated every a few angles and X-ray beams are transmitted through the target sample. Absorption of X-ray beams occurs and is used to provide a 3D representation of the rock and fluids. The details can be referred to (Heindel, 2011; Blunt et al., 2013; Wildenschild and Sheppard, 2013) the series of 3D tomographic images are then reconstructed from a stack of two-dimensional (2D) radiograph projections taken at different angles (Sakellariou et al., 2004; Varslot et al., 2011). Before image data processing, it is necessary to check whether any artifacts exist in the tomograms. Preilters before image processing are commonly used because the reconstructed 3D tomographic images are inherently associated with noises, which has a relationship with the noise in the X-ray intensity measurements (Nishiki et al., 2008). Filters such as image noise reduction and phase boundary sharpen are needed as well as ring artefacts for image enhancement (Pratt, 1991; Sheppard et al., 2004; Blunt et al., 2013). In this review, we will not present details for the techniques of image enhancement.

Image processing for multiphase images includes image registration and segmentation. Image registration refers to the alignment of one image dataset with another. For multiphase images that obtained by imaging scanning at different time steps, image registration technique provides aligning wet images with respect to dry images, which allows observing and locating fluid configuration before and after flooding taken at any times. Registration of two images requires a comprehensive search along the entire image dataset for its match on the fixed image. It is based on similarity-based optimization techniques and the detail can be referred to. An example of 3D multiphase image registration is shown in Fig. 1. Afterwards, the registered wet images are ready for segmentation for all phases present in porous media and further image-based qualification and analysis image. Segmentation means to identify which phase each voxel belongs to (Sheppard et al., 2004). Compared with dry image, segmentation for wet images is more complicated due to the ambiguity associated with solid phase. The optimal workflow for segmentation of partially saturated two-phase images is briefly described

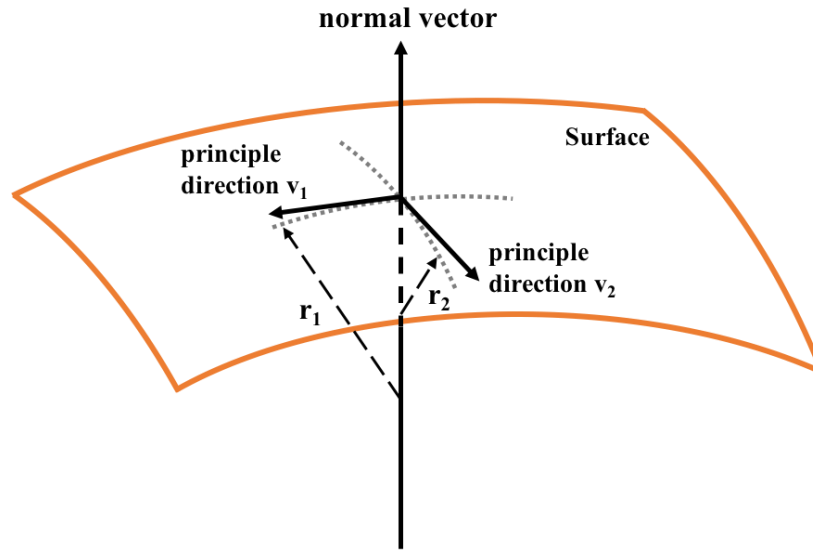


Fig. 2. A small expansion of an interface between two liquids. Two principal radii of curvature are r_1 and r_2 are illustrated in the figure allowing the Young-Laplace equation to be derived (reproduced from (Armstrong et al., 2012; Li et al., 2018).

to firstly segment dry image into solid and void space by using a standard watershed algorithm (Sheppard et al., 2014). Afterwards, multiphase images are firstly segmented for one fluid phase in the pore space. Next, the registered segmented dry image and wet images segmented with one fluid phase are used to mask out the other fluid and solid phase in the wet images. Finally, the partially saturated images can be segmented clearly for all phases present in the core.

4. Image data qualification and analysis

4.1 Porosity, saturation, and absolute permeability

Based on the dry segmented image, the porosity can be determined by the portion of void phase in porous media. Similarly, for wet segmented images, simple voxel counting is used to measure fluid saturations (i.e., wetting phase S_w and residual nonwetting phase saturations S_{nw}). The saturation of water and oil is computed from the segmented images at each time step. Absolute permeability can be directly computed in the pore space by numerical methods. The workflow to compute absolute permeability is to discretize the void space from a binarized 3D image and then numerical simulations are run to determine absolute permeability (Blunt et al., 2013). One example of absolute permeability computations can be referred to (Mostaghimi et al., 2013).

4.2 Interfacial area and curvature of fluids

The advent of pore-scale multiphase imaging potentially offers a flexible and powerful approach for the measurement of interfacial area which can be computed from segmented images of the pore space and the fluid phases (Blunt, 2017). To compute the interfacial areas, the interface between fluid/fluid phases, which are smoothed to avoid voxelization artefacts, is firstly extracted. The resulting surfaces are used to compute

the specific interfacial area between oil and water (interfacial area per unit volume). For instance, when measuring water/oil interfacial area in a water-oil system, all the phase boundaries are firstly extracted, i.e., water/oil, water/rock and water/rock. Then a boundary-preserving surface smoothing algorithm is applied. It shifts the vertices of the original voxelized images such that each vertex is moved towards the average position of its neighbors. The water/oil phase boundary is then isolated from the rest. The interfacial area is calculated by measuring the surface area labeled as the water/oil interface (Schlüter et al., 2016).

The curvature of the interface leads to a pressure difference between the phases. Pressure differences across a curved interface separating two immiscible fluid is capillary pressure (P_c) which is defined as:

$$P_c = P_o - P_w \quad (1)$$

where the subscripts o , w refer to the oleic phase and the water phase, respectively. Capillary pressure is an inherently a pore-scale parameter, which at equilibrium is related to interfacial curvature by the Young-Laplace equation

$$P_c = 2\sigma k \quad (2)$$

$$\kappa = \frac{1}{2}(k_1 + k_2) \quad (3)$$

where σ is the interfacial tension between the immiscible phases, k is the mean curvature, and k_1 , k_2 are the two principal curvatures of the surface. The schematic of curvature is illustrated as Fig. 2.

Fluid/fluid interfacial curvatures within 3D porous media systems can be quantified directly from X-ray microcomputed tomographic images at the pore-scale and equating this curvature with Young-Laplace capillary pressure equation (Hassanizadeh and Gray, 1993). Armstrong et al. (2012) used the Young-Laplace equation to measure 3D curvatures and

correlated with transducer-based capillary pressure up to approximately 300 Pa for water/oil interfaces in glass bead packs. Following this, studies have been carried out to measure fluid curvatures and then correlate it to capillary pressure (Herring et al., 2017; Li et al., 2018). Sun et al. (2020c) recently extracted the Gaussian curvatures from the capillary pressure data and then used the distribution to predict the *in situ* contact angle by applying the Gauss-Bonnet theorem.

To estimate the interfacial curvatures of fluids, isosurfaces are constructed between fluid/fluid interfaces from the segmented images. Triangulation of the surface is performed by applying surface mesh generating techniques such as marching cubes algorithm. Then curvatures are constructed locally on the triangulated interfacial surface as a quadratic form and the eigenvalues and eigenvectors of the quadratic form represent the magnitude and the direction of principal curvatures, respectively. This produces a surface scalar field that contains the mean value of the two principal curvature values, as used for Young-Laplace equation.

4.3 Wettability in porous media

For multiphase flow, wettability characterization by contact angle is based on segmented pore-scale images acquired from multiphase flow experiments.

4.3.1 Contact angle measurements using energy and force balance

A thermodynamic method that relies on the 3D X-ray micro-computed tomography imaging technology to track the fluid interface can be applied to characterize the wetting state of the bulk multiphase system. Blunt et al. (2019) proposed a thermodynamic method that follows the work of Morrow (1970) based on the conservation law and derives a thermodynamically-consistent contact angle to represent the wettability of the whole system. The thermodynamic contact angle considers the changes in fluid interfacial area and phase saturation. In their study, the approach assumes a local equilibrium state of the system and energy dissipation in the system during dynamic fluid displacement events is neglected. Therefore, the contribution of these dynamic effects to the resulting contact angles are disregarded. Recent studies (Seth and Morrow, 2006; Berg et al., 2013) have shown that there exists a considerable large amount of energy dissipation that would be expected for various type of rocks during fluid displacement events, i.e., imbibition and drainage processes. As a consequence, the derived thermodynamic contact angle underestimates the wetting state of the bulk system. In their following work, they showed the thermodynamic contact angle provides a reasonable estimation of a representative wetting state on a pore-by-pore basis under the condition where the displacement events cause less viscous dissipation (Akai et al., 2020). It is suitable for cases such as water flooding in water-wet and mixed-wet porous media under the situations where the effects of viscous dissipation are minimal. However, for rapid pore filling events in the drainage processes, the viscous dissipation due to displacement mechanism cannot be

disregarded. The contact angle can be determined from force-based approach based on the threshold capillary pressure by assuming an axi-symmetric fluid interface as developed by (Mascini et al., 2020). The force-based contact angle (θ_f) can be derived from Young-Laplace equation by

$$P_c = 2\sigma K_{thr} = \frac{2\sigma \cos \theta_f}{r} \quad (4)$$

where P_c represents the capillary pressure, r represents pore throat radius and K_{thr} is threshold curvature in the pore throat. σ is the interfacial tension between the immiscible fluids. Finally, the force-based contact angle can be obtained in terms of Eq. (4)

$$\theta_f = \arccos(K_{thr}r) \quad (5)$$

4.3.2 Contact Angle Measurements using Direct Local Methods

In addition to estimate thermodynamically-consistent contact angle using energy balance, the advent of high/micron-resolution imaging technology has made it possible to measure the *in situ* contact angles locally along the three-phase contact line. The 2D local method is performed by fitting a circle on the fluid/fluid interface and a line to the fluid/solid interface on 2D slices of segmented micro-CT images that perpendicular to the contact line (Scanziani et al., 2017). Sun et al. (2020b) applied the 2D local method to measure the contact angle at each three-phase contact point by extending the work of (Scanziani et al., 2017).

For the extended 2D local method as shown in Fig. 3, the contact points were smoothed using a moving average to determine the position and direction of the contact line. A 2D image was then extracted normal to the direction of the contact line for each contact point. In addition, a constant curvature was assumed, and a circular regression was applied for the fluid/fluid interface under the assumption that the system is at equilibrium condition. As shown in Fig. 3, both circular and linear regressions were applied to best fit the solid surface. The choice depends on the root mean square error (RMSE) of the best fit for the solid surface. If the circle approximation was selected as the best fit, a line tangent to the circle at the contact point was calculated to represent the slope of the surface at that point. Consequently, the apparent contact angle was measured as the angle between the solid surface and liquid/vapor interface tangent lines.

AlRatrouf et al. (2017) developed an approach to measure the contact angles at the pore-scale automatically. Other than fitting lines and planes to fluid interface in the segmented image, it discretizes the fluid/fluid and fluid/solid interfaces and define vectors that have a direction perpendicular to these interfaces. Two vectors (n_{ff} and n_{fs}) that have a direction perpendicular to both fluid/fluid and fluid/solid interface and their resulting angle were measured for each contact point along the three-phase contact line.

4.3.3 Contact Angle Measurements using Deficit Curvature

To address the issue of contact angle hysteresis and provide

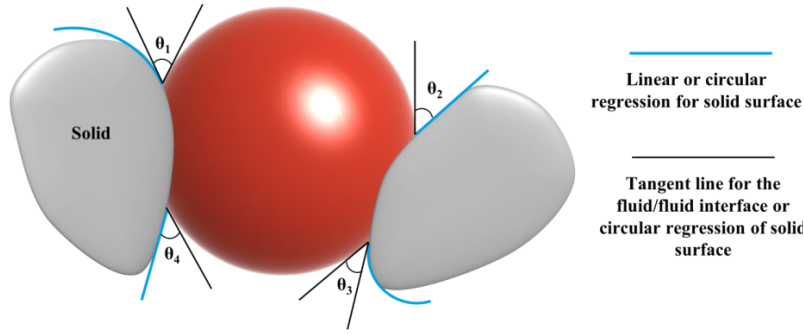


Fig. 3. The schematic illustration of 2D local method for measuring contact angle directly at each three-phase contact points for a fluid droplet (red color). The solid (grey color) surface is fitted by either linear regression or circular regression, which depends on the root mean square error of the best fit.

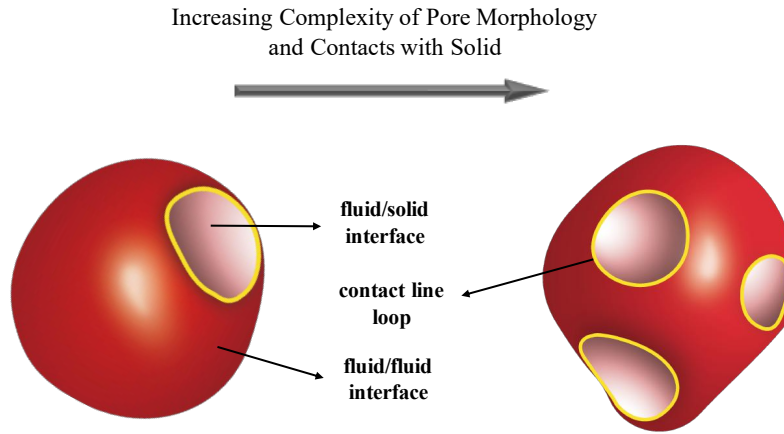


Fig. 4. The schematic illustration of wettability characterization by applying principles of topological and integral geometry. From left to right, there is an increase in pore morphology complexity and contacts with the solid (Sun et al., 2020a).

a macroscopic wetting information where direct numerical simulation benefits, Sun et al. (2020b) proposed a method by using the principles of topological and integral geometry. The Gauss-Bonnet theorem is applied by linking the total Gaussian curvature of the bulk topology of fluid droplets to the Euler characteristic. The Euler characteristic for a topological space (X) is a topological invariant and can be defined as,

$$\chi(X) = N - \mathcal{C} + \mathcal{O} \quad (6)$$

where N is the number of isolated elements or isolated convex, i.e., oil blobs; \mathcal{O} is the number of enclosed elements or closed concave, i.e., trapped oil drop by other fluids; \mathcal{C} is the number of redundant connection between the oil blobs.

Fig. 4 shows the fluid droplets that have an Euler characteristic of one where there is an increase in pore morphology complexity and contacts with the solid from left to right. The Gauss-Bonnet theorem states that the Euler characteristic (χ) is constant when the interface of a 3D fluid droplet (D) is closed and has the same structure regardless of the way it is bent, which can be written as

$$4\pi\chi(D) = \int k_G dA + \int k_g dC \quad (7)$$

where dA and dC are the droplet interfacial area element along the surface and the line element along the contact line,

respectively. k_G and k_g are Gaussian curvatures along the droplet interface and the geodesic curvature along the contact line, respectively. The geodesic curvature term $\int k_g dC$ is the curvature of the projection of the contact line on to the tangent plane to the droplet interface. It can be separated relative to the fluid/fluid interface (ff) and fluid/solid (fs) interface, which can be expressed as

$$\int k_g dC = \int (k_{g_{ff}} + k_{g_{fs}}) dC \quad (8)$$

Deficit curvature, which is defined as the summation of geodesic curvatures along the contact line as shown in Eq. (8). When the droplet contacts with the solids, there are some curvatures being deficit, and the lost curvature will redistribute along the contact line. Therefore, it corresponds to a total contact angle of change due to the wetting behavior of the system. The macroscopic contact angle (θ^m) can finally be obtained by normalizing the deficit curvature with the number of contact line loop (N_c) for the droplet (Sun et al., 2020a, 2020b), which can be expressed as,

$$\theta^m = \lambda \frac{\int k_g dC}{N_c} \quad (9)$$

where λ is a scale factor to impose θ^m to fall in the range between 0° and 180° , which ensures it is consistent with

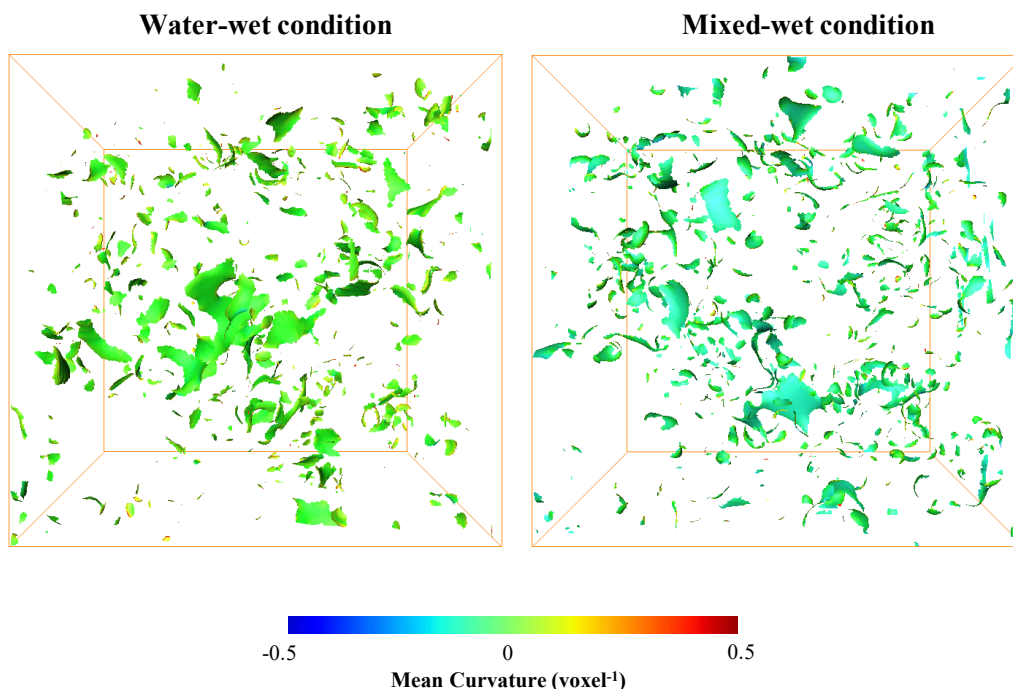


Fig. 5. The oil/brine interfaces obtained from segmented images of portions of the rock for North Sea sandstone, which shows the water-wet case (left) and the mixed-wet case (right). In the water-wet case, the mean curvature is mostly positive, while for the mixed-wet rock, the mean curvature is close to zero, showing the well-connected fluid interfaces.

the conventional wetting metric (Sun et al., 2020a).

5. Wettability effect on multiphase flow

Wettability plays a significant role in multiphase flow in porous media since it controls the location, spatial distribution and flow of fluids in porous media (Anderson, 1987; Li and Hou, 2019). Direct imaging for fluid distribution in porous media by combining multiphase flow experiments with *in situ* imaging scanning provides a promising way to characterize the impact of wettability on multiphase flow through observing fluid distributions before and after flooding (Karpyn et al., 2010; Landry et al., 2011; Wildenschild et al., 2011; Iglauer et al., 2012; Kumar et al., 2012; Celauro et al., 2014; Murison et al., 2014; Setiawan et al., 2014).

Singh et al. (2016) altered the wettability of the carbonate rock from water-wet to mixed-wet and investigated the impact of wettability on the pore-scale spatial fluid distribution in the same rock. By imaging the remained oil distribution with different water fractional flows at ambient pressure, pore-scale multiphase images provide direct visualization for continuous pathway layers for slow oil drainage in a mixed-wet system (Salathiel, 1973; Kovscek et al., 1993). The quantitative analysis from imaged fluid distribution shows that remaining oil saturation in a water-wet system is about two times larger than that obtained in the mixed-wet rock, while the measured water/oil interfacial area is three times smaller than that of oil layers in mixed-wet system.

Zou et al. (2018) imaged fluid distributions on a water-wet and altered-wet sandstone at decreasing water fractional flows during two-phase drainage steady state flow. Pore-scale

images show that with original water-wet sandstone altered to mixed-wet condition, more oil is flooded into pore space at the same injection ratio, demonstrating experimental evidence for wettability effect on oil distribution. From multiphase images taken at different water fractional flow, since partial pores are altered to oil-wet in the mixed-wet system, more oil can reach narrow pores that are not accessible to oil phase in the water-wet core until higher capillary pressure is reached. Lin et al. (2019) performed two-phase imbibition experiments on a water-wet and altered-wet sandstone under steady state. Pore-scale multiphase images under different fluid saturations were acquired, allowing interfacial area, curvatures, and contact angles to be calculated directly on imaged fluid distributions. Their results demonstrated that with wettability alteration from water-wet to mixed-wet, the measured contact angles are roughly 80° and the fluid interfacial area shows largely constant values. For the water-wet sample, the mean curvature is positive and oil bulges into the brine with almost spherical interfaces. In the mixed-wet case, the mean curvature is close to zero while the curvature in one direction shows almost equal value but opposite in sign to the curvature in a perpendicular direction. From images as shown in Fig. 5, the distribution of fluid curvatures are observed to be approximately minimal surfaces, which implies well-connected phases in mixed-wet condition (Blunt et al., 2019; Scanziani et al., 2020). Thus, capillary pressure measured from interfacial curvature is calculated to be a small value and approximately constant over a wide range of saturation compared with that measured on a similar water-wet rock.

6. Discussion, conclusion and outlook

This paper reviews recent studies on the application of X-ray imaging technique to characterize wetting state for multiphase flow and related transport in porous media. The main limitation of this technique is only the small volume of core sample can be imaged with micro-scale resolution for pore-scale as the higher resolution can resolve more fine analysis. For two-phase flow mechanisms, the issue of representative element volume (REV) remains an open question for pore-scale analysis conducted on multiphase images. Another issue is that X-ray imaging technique cannot fully resolve micropores or the mineralogy existing in the pore space, which may affect the accuracy for spatial characterization of fluid distributions in natural porous media.

The images experimentally obtained provide *in situ* multiphase flow distributions and allow a complete information of interfacial areas, curvatures, and contact angles inferred from multiphase images. However, wettability parameters determined from pore scale multiphase images such as contact angle, curvature and interfacial areas measurements which are based on interfaces to voxelized pore scale images are largely susceptible to errors due to image quality and pixelation-related segmentation errors and ultimately, these systematic errors complicate the process of quantifying the wetting state of a porous multiphase system. For instance, contact angle measurement computed by the local method is depended on the identification of the three-phase contact line and measurement of an angle over a few voxels which is inherently error-prone. Another issue is that broad distributions of wetting parameters measured at different locations for the images, i.e., the advancing and receding angles, is observed along the contact line in porous systems due to surface heterogeneity. This spatial variation of contact angles only provides the phenomenological information for technological processes and triggers great difficulty in characterizing wettability of the system for the porous media system.

Further works can be focused on intergrating wetting parameters that are inferred from multiphase images into pore-scale models, allowing a pore-by-pore comparison between imaged and simulated fluid distribution and furthermore simulation at larger scale capable of capturing heterogeneity in core samples. For instance, how the wetting parameters obtained at micro-scale impacts core-scale flow properties, such as relative permeability and capillary pressure/saturation functions, should be emphasized in details. Moreover, we could also extend X-ray micro-computed tomography experiments to investigate different types of rock sample at reservoir conditions, including carbonates and unconventional shale samples under high pressure, temperature and other relevant variables conditions.

Acknowledgement

Shuangmei Zou would like to acknowledge the Fundamental Research Funds for the Central Universities (No. CUGGC04).

Conflict of interest

The authors declare no competing interest.

Open Access This article is distributed under the terms and conditions of the Creative Commons Attribution (CC BY-NC-ND) license, which permits unrestricted use, distribution, and reproduction in any medium, provided the original work is properly cited.

References

- Akai, T., Lin, Q., Bijeljic, B., et al. Using energy balance to determine pore-scale wettability. *J. Colloid Interface Sci.* 2020, 576: 486-495.
- AlRatrou, A., Raeni, A.Q., Bijeljic, B., et al. Automatic measurement of contact angle in pore-space images. *Adv. Water Resour.* 2017, 109: 158-169.
- Anderson, W.G. Wettability literature survey part 5: The effects of wettability on relative permeability. *J. Pet. Technol.* 1987, 39(11): 1453-1468.
- Andrew, M., Bijeljic, B., Blunt, M.J. Pore-scale contact angle measurements at reservoir conditions using X-ray microtomography. *Adv. Water Resour.* 2014, 68: 24-31.
- Armstrong, R.T., McClure, J.E., Berrill, M.A., et al. Beyond Darcy's law: The role of phase topology and ganglion dynamics for two-fluid flow. *Phys. Rev. E* 2016, 94(4): 043113.
- Armstrong, R.T., Porter, M.L., Wildenschild, D. Linking pore-scale interfacial curvature to column-scale capillary pressure. *Adv. Water Resour.* 2012, 46: 55-62.
- Berg, S., Ott, H., Klapp, S.A., et al. Real-time 3D imaging of Haines jumps in porous media flow. *Proc. Natl. Acad. Sci.* 2013, 110(10): 3755-3759.
- Blunt, M.J. *Multiphase Flow in Permeable Media: A Pore-Scale Perspective*. Cambridge, UK, Cambridge University Press, 2017.
- Blunt, M.J., Bijeljic, B., Dong, H., et al. Pore-scale imaging and modelling. *Adv. Water Resour.* 2013, 51: 197-216.
- Blunt, M.J., Lin, Q., Akai, T., et al. A thermodynamically consistent characterization of wettability in porous media using high-resolution imaging. *J. Colloid Interface Sci.* 2019, 552: 59-65.
- Celauro, J.G., Torrealba, V., Karpyn, Z., et al. Pore-scale multiphase flow experiments in bead packs of variable wettability. *Geofluids* 2014, 14(1): 95-105.
- Coles, M., Hazlett, R., Spanne, P., et al. Pore level imaging of fluid transport using synchrotron X-ray microtomography. *J. Pet. Sci. Eng.* 1998, 19(1-2): 55-63.
- Feali, M., Pinczewski, V., Cinar, Y., et al. Qualitative and quantitative analyses of the three-phase distribution of oil, water, and gas in Bentheimer sandstone by use of micro-CT imaging. *SPE Reserv. Eval. Eng.* 2012, 15: 706-711.
- Gao, Y., Lin, Q., Bijeljic, B., et al. X-ray microtomography of intermittency in multiphase flow at steady state using a differential imaging method. *Water Resour. Res.* 2017, 53(12): 10274-10292.
- Georgiadis, A., Berg, S., Makurat, A., et al. Pore-scale micro-computed-tomography imaging: Nonwetting-phase cluster-size distribution during drainage and imbibition.

- Phys. Rev. E 2013, 88(3): 033002.
- Hassanizadeh, S.M., Gray, W.G. Thermodynamic basis of capillary pressure in porous media. *Water Resour. Res.* 1993, 29(10): 3389-3405.
- Heindel, T.J. A review of X-ray flow visualization with applications to multiphase flows. *J. Fluids Eng.* 2011, 133(7): 074001.
- Herring, A.L., Middleton, J., Walsh, R., et al. Flow rate impacts on capillary pressure and interface curvature of connected and disconnected fluid phases during multiphase flow in sandstone. *Adv. Water Resour.* 2017, 107: 460-469.
- Hussain, F., Pinczewski, W.V., Cinar, Y., et al. Computation of relative permeability from imaged fluid distributions at the pore scale. *Transp. Porous Media* 2014, 104(1): 91-107.
- Iglauer, S., Fernø, M., Shearing, P., et al. Comparison of residual oil cluster size distribution, morphology and saturation in oil-wet and water-wet sandstone. *J. Colloid Interface Sci.* 2012, 375(1): 187-192.
- Karpyn, Z.T., Piri, M., Singh, G. Experimental investigation of trapped oil clusters in a water-wet bead pack using X-ray microtomography. *Water Resour. Res.* 2010, 46(4): W04150.
- Kovscek, A.R., Wong, H., Radke, C.J. A pore-level scenario for the development of mixed wettability in oil reservoirs. *AIChE J.* 1993, 39(6): 1072-1085.
- Kumar, M., Fogden, A., Senden, T., et al. Investigation of pore-scale mixed wettability. *SPE J.* 2012, 17(1): 20-30.
- Landry, C.J., Karpyn, Z.T., Piri, M. Pore-scale analysis of trapped immiscible fluid structures and fluid interfacial areas in oil-wet and water-wet bead packs. *Geofluids* 2011, 11(2): 209-227.
- Li, J., Jiang, H., Wang, C., et al. Pore-scale investigation of microscopic remaining oil variation characteristics in water-wet sandstone using CT scanning. *J. Nat. Gas Sci. Eng.* 2017, 48: 36-45.
- Li, S., Hou, S. A brief review of the correlation between electrical properties and wetting behaviour in porous media. *Capillarity* 2019, 2(3): 53-56.
- Li, T., Schlüter, S., Dragila, M.I., et al. An improved method for estimating capillary pressure from 3D microtomography images and its application to the study of disconnected nonwetting phase. *Adv. Water Resour.* 2018, 114: 249-260.
- Lin, Q., Bijeljic, B., Berg, S., et al. Minimal surfaces in porous media: Pore-scale imaging of multiphase flow in an altered-wettability Bentheimer sandstone. *Phys. Rev. E* 2019, 99(6): 063105.
- Mascini, A., Cnudde, V., Bultreys, T. Event-based contact angle measurements inside porous media using time-resolved micro-computed tomography. *J. Colloid Interface Sci.* 2020, 572: 354-363.
- Morrow, N.R. Physics and thermodynamics of capillary action in porous media. *Ind. Eng. Chem.* 1970, 62(6): 32-56.
- Mostaghimi, P., Blunt, M.J., Bijeljic, B. Computations of absolute permeability on micro-CT images. *Math. Geosci.* 2013, 45(1): 103-125.
- Murison, J., Semin, B., Baret, J.C., et al. Wetting heterogeneities in porous media control flow dissipation. *Phys. Rev. Appl.* 2014, 2(3): 034002.
- Nishiki, M., Shiraishi, K., Sakaguchi, T., et al. Method for reducing noise in X-ray images by averaging pixels based on the normalized difference with the relevant pixel. *Radiol. Phys. Technol.* 2008, 1(2): 188-195.
- Pratt, W.K. *Digital Image Processing*. New York, USA, John Wiley & Sons, 1991.
- Reynolds, C., Krevor, S. Characterizing flow behavior for gas injection: Relative permeability of CO₂-brine and N₂-water in heterogeneous rocks. *Water Resour. Res.* 2015, 51(12): 9464-9489.
- Reynolds, C.A., Menke, H., Andrew, M., et al. Dynamic fluid connectivity during steady-state multiphase flow in a sandstone. *Proc. Natl. Acad. Sci.* 2017, 114(31): 8187-8192.
- Rücker, M., Bartels, W.B., Singh, K., et al. The Effect of mixed wettability on pore-scale flow regimes based on a flooding experiment in Ketton Limestone. *Geophys. Res. Lett.* 2019, 46(6): 3225-3234.
- Sakellariou, A., Sawkins, T., Senden, T., et al. X-ray tomography for mesoscale physics applications. *Phys. A* 2015, 339(1-2): 152-158.
- Salathiel, R.A. Oil recovery by surface film drainage in mixed-wettability rocks. *J. Pet. Eng. Technol.* 1973, 25(10): 1216-1224.
- Scanziani, A., Lin, Q., Alhosani, A., et al. Dynamics of displacement in mixed-wet porous media. *Proc. R. Soc. A* 2020, 476: 20200040.
- Scanziani, A., Singh, K., Blunt, M.J., et al. Automatic method for estimation of *in situ* effective contact angle from X-ray micro tomography images of two-phase flow in porous media. *J. Colloid Interface Sci.* 2017, 496: 51-59.
- Schlüter, S., Berg, S., Rücker, M., et al. Pore-scale displacement mechanisms as a source of hysteresis for two-phase flow in porous media. *Water Resour. Res.* 2016, 52(3): 2194-2205.
- Seth, S., Morrow, N.R. Efficiency of conversion of work of drainage to surface energy for sandstone and carbonate. Paper SPE 102490 Presented at the SPE Annual Technical Conference and Exhibition, San Antonio, Texas, USA, 24-27 September, 2006.
- Setiawan, A., Suekane, T., Deguchi, Y., et al. Three-dimensional imaging of pore-scale water flooding phenomena in water-wet and oil-wet porous media. *J. Flow Control, Meas. Visualization* 2014, 2(2): 25-31.
- Sheppard, A., Latham, S., Middleton, J., et al. Techniques in helical scanning, dynamic imaging and image segmentation for improved quantitative analysis with X-ray micro-CT. *Nucl. Instrum. Methods Phys. Res. B* 2014, 324: 49-56.
- Sheppard, A.P., Sok, R.M., Averdunk, H. Techniques for image enhancement and segmentation of tomographic images of porous materials. *Phys. A* 2004, 339(1-2): 145-151.
- Singh, K., Bijeljic, B., Blunt, M.J. Imaging of oil layers, curvature and contact angle in a mixed-wet and a water-wet carbonate rock. *Water Resour. Res.* 2016, 52(3):

- 1716-1728.
- Sun, C., McClure, J.E., Mostaghimi, P., et al. Probing effective wetting in subsurface systems. *Geophys. Res. Lett.* 2020a, 47(5): e2019GL086151.
- Sun, C., McClure, J.E., Mostaghimi, P., et al. Characterization of wetting using topological principles. *J. Colloid Interface Sci.* 2020b, 578: 106-115.
- Sun, C., McClure, J.E., Mostaghimi, P., et al. Linking continuum-scale state of wetting to pore-scale contact angles in porous media. *J. Colloid Interface Sci.* 2020c, 561: 173-180.
- Turner, M., Knuefing, L., Arns, C., et al. Three-dimensional imaging of multiphase flow in porous media. *Phys. A* 2004, 339(1-2): 166-172.
- Varslot, T., Kingston, A., Myers, G., et al. High-resolution helical cone-beam micro-CT with theoretically-exact reconstruction from experimental data. *Med. Phys.* 2011, 38: 5459.
- Wildenschild, D., Armstrong, R.T., Herring, A.L., et al. Exploring capillary trapping efficiency as a function of interfacial tension, viscosity, and flow rate. *Energy Procedia.* 2011, 4: 4945-4952.
- Wildenschild, D., Sheppard, A.P. X-ray imaging and analysis techniques for quantifying pore-scale structure and processes in subsurface porous medium systems. *Adv. Water Resour.* 2013, 51: 217-246.
- Youssef, S., Bauer, D., Bekri, S., et al. 3D *In-situ* fluid distribution imaging at the pore scale as a new tool for multiphase flow studies. Paper SPE 135194 Presented at SPE Annual Technical Conference and Exhibition, Florence, Italy, 19-22 September, 2010.
- Zou, S., Armstrong, R.T., Arns, J.Y., et al. Experimental and theoretical evidence for increased ganglion dynamics during fractional flow in mixed-wet porous media. *Water Resour. Res.* 2018, 54(5): 3277-3289.